Incorporating uplift in the analysis of shallowly embedded pipelines

Yinghui Tian[a] and Mark J. Cassidy*

*Centre for Offshore Foundation Systems, The University of Western Australia,
35 Stirling Highway, Crawley WA 6009, Australia*

Abstract. Under large storm loads sections of a long pipeline on the seabed can be uplifted. Numerically this loss of contact is extremely difficult to simulate, but accounting for uplift and any subsequent recontact behaviour is a critical component in pipeline on-bottom stability analysis. A simple method numerically accounting for this uplift and reattachment, while utilising efficient force-resultant models, is provided in this paper. While force-resultant models use a plasticity framework to directly relate the resultant forces on a segment of pipe to the corresponding displacement, their historical development has concentrated on precisely modelling increasing capacity with penetration. In this paper, the emphasis is placed on the description of loss of penetration during uplifting, modelled by 'strain-softening' of the force-resultant yield surface. The proposed method employs uplift and reattachment criteria to determine the pipe uplift and recontact. The pipe node is allowed to become free, and therefore, the resistance to the applied hydrodynamic loads to be redistributed along the pipeline. Without these criteria, a localised failure will be produced and the numerical program will terminate due to singular stiffness matrix. The proposed approach is verified with geotechnical centrifuge results. To further demonstrate the practicability of the proposed method, a computational example of a 1245 m long pipeline subjected to a large storm in conditions typical of offshore North-West Australia is discussed.

Keywords: pipeline; soil-structure interaction; centrifuge test; calcareous sand; force-resultant model; plasticity

1. Introduction

For offshore pipelines laid on the seafloor, one of the most fundamental engineering tasks is to ensure their on-bottom stability under the action of hydrodynamic loads due to waves and currents. In many offshore engineering projects around the world, pipeline stabilisation is a major cost driver. A typical example is the developing North West Shelf of Australia, where shallow water, complex calcareous soil conditions and severe environmental loading from summer tropical cyclones are providing a challenging environment for pipeline stability. In large cyclones unburied pipelines are subjected to large uplift forces. The possible detachment of the pipe from the seabed and the loss of soil resistance can cause large lateral movements greater than the acceptable design criteria. In such

---

*Corresponding author, Professor, E-mail: mcassidy@civil.uwa.edu.au
[a]Research Associate, E-mail: tian@civil.uwa.edu.au

circumstance the use of secondary stabilisation, such as anchors or rock dump, can represent as much as 30% of the total pipeline capital expenditure (Brown *et al.* 2002). This provides the incentive for development of more accurate analysis and design methods. This paper discusses methods that enable the prediction of the movement of long pipelines in large storms.

Traditional pipeline stability design approaches, such as those found in early design codes (e.g., Det Norske Veritas 1981), use the simplistic Coulomb friction model to describe pipe-soil behaviour and adopt force balance methods to ensure a small plane-strain pipe section does not displace horizontally. More recent updates, such as the Det Norske Veritas DNV-RP-E305 (Det Norske Veritas 1988) and DNV-RP-F109 (Det Norske Veritas 2007), retain simplistic stability methods, but also encourage users to perform dynamic three-dimensional stability analyses under hydrodynamic loads. Although recommended for some time, and considered the most comprehensive method, dynamic three-dimensional modelling is still not widely adopted in practice. Tørnes *et al.* (2009) believes this is due to availability and limitations of numerical analysis software. In addition to the pioneering dynamic programs directly derived from Joint Industry Projects, namely the AGA software package and PONDUS (Holthe *et al.* 1987, PRCI 2002), a few more time domain dynamic programs have emerged in recent years, for example the SimStab (Tørnes *et al.* 2009, Zeitoun *et al.* 2009) and UWA ABAQUS based codes (Tian *et al.* 2010b, Youssef *et al.* 2010).

A key issue for the comprehensive dynamic lateral stability analysis of unburied pipelines is employment of a realistic and efficient pipe-soil interaction model. In addition to the traditional empirically based models, such as Wantland *et al.* (1979), Brennodden *et al.* (1989), Wagner *et al.* (1989), Verley and Sotberg (1992) and Verley and Lund (1995), force-resultant models based on plasticity theory (such as Zhang 2001, Calvetti *et al.* 2004, Di Prisco *et al.* 2004, Hodder and Cassidy 2010, Tian *et al.* 2010a, Tian and Cassidy 2011b) are becoming an attractive option to describe the pipe-soil interaction behaviour. These models provide a more fundamental understanding of the pipe-soil mechanism, as highlighted by Cathie *et al.* (2005) and Zeitoun *et al.* (2008). These force-resultant models directly relate the resultant vertical and horizontal forces on a segment of pipe to the corresponding displacement. As plasticity models are expressed in a terminology consistent with pipeline structural analysis, multiple force-resultant models can be incorporated as single node elements in a long pipeline structural analysis (see Cassidy 2006, Tian and Cassidy 2008, 2010 for details). This facilitates three-dimensional time domain dynamic lateral stability analysis of a long pipeline subjected to random storm waves.

As illustrated in Fig. 1, pipelines laid on the seabed are subjected to a combination of horizontal (F_H) and uplift (F_L) hydrodynamic forces. Under extremely large storm loads, when the lift force (F_L) is approaching or greater than the submerged self-weight (W_s), sections of a long pipeline can be uplifted. Accurately modelling this loss of penetration, and then setting a criterion to predict uplift off the seabed, are becoming critical components as long as the dynamic lateral stability analysis is to be used. Unfortunately, the development of pipe-soil force-resultant models has also concentrated on precisely modelling increasing capacity with penetration. This is because models now used for pipelines initiated from similar plasticity based models for mobile 'jack-up' platform footings (see Schotman 1989, Martin and Houlsby 2001, Houlsby and Cassidy 2002, Cassidy *et al.* 2002, 2004, Bienen *et al.* 2006, Bienen and Cassidy 2009, Cassidy 2011 for example), where the size of an expanding yield surface was experimentally measured as a function of the footing's plastic vertical penetration (Gottardi *et al.* 1999, Martin and Houlsby 2000, Cassidy 2007, Gaudin *et al.* 2011).

During the time domain dynamic lateral stability analysis of a pipeline, uplift and reattachment

becomes a possible, if not common, scenario. Therefore, a criterion is required and a numerical methodology needs to be introduced to allow the pipe-soil model to 'detach' from the seabed and numerically become inactive under the uplifting loads. During loss of penetration the force-resultant model's yield surface and thus stiffness matrix degrades until almost zero. At this point it can be considered as lifted off the seabed. This allows the numerical analysis to continue and the hydrodynamic forces on the 'detached' pipe to shed to neighbouring elements located within the soil. Without this criterion, the pipe-soil model will predict a "failure" at one segment of the pipe and the dynamic time domain analysis cannot finish the full storm time series due to an ill conditioned stiffness matrix.

This paper also introduces a strategy to numerically reattach the pipe elements if the pipe returns to the seabed. One scenario is that the pipe recontacts the seabed close to the original uplift point in a region where the soil has been previously loaded. The other scenario is when the pipeline has been displaced a significant distance above the seabed. On reattachment, the segment of the pipe touches a seabed unaffected by the original activity.

This paper has three goals. Firstly, the methodology to account for both uplift and reattachment of pipes is demonstrated with a two-surface kinematic hardening force-resultant model describing the behaviour of a pipe segment in calcareous sands. Secondly, centrifuge tests are used to verify the lift behaviour and the numerical criterion. Finally, an example of a 1245 m long pipeline analysis highlights the significance of the uplift and reattachment criterion in a time domain dynamic lateral analysis.

2. Force-resultant modelling and implementation of the UWAPIPE model

The pipe-soil interaction model used in this paper was initially developed by Zhang (2001) and Zhang *et al.* (2002a, b) and its use has also been recommended in DNV-RP-F109 (Det Norske Veritas 2007). Recently it has been slightly modified and named the UWAPIPE model by Tian and Cassidy (2008a). The force-resultant UWAPIPE model uses a plasticity framework to directly relate
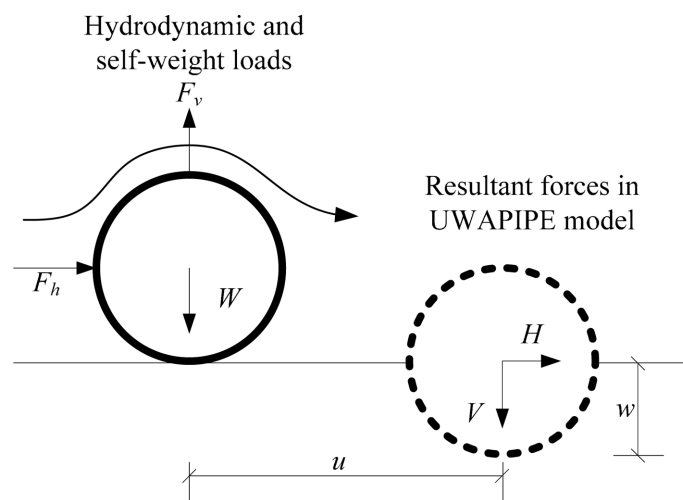

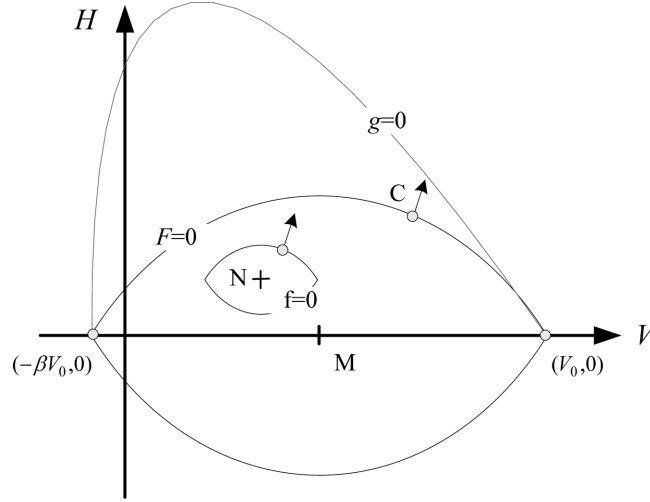Fig. 1 Forces on pipe segment and sign convention adopted

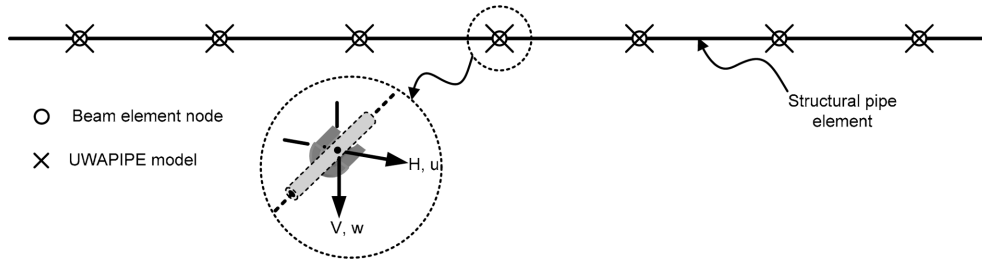Fig. 2 UWAPIPE model illustration (see Appendix for symbol definition)

Fig. 3 Incorporation of force-resultant UWAPIPE model into a structural finite element program

the resultant forces (V, H) on a segment of pipe to the corresponding displacement (w, u). The sign convention adopted in this paper is shown in Fig. 1.

A brief review of the numerical formulation of the UWAPIPE model is provided in the Appendix, with full details available in Tian and Cassidy (2008a, 2010). Based within the framework of conventional two-surface isotropic and kinematic hardening plasticity theory, the UWAPIPE model comprises of an outer bounding surface (written directly in load space), an inner yield or "bubble" surface, isotropic and kinematic hardening laws, a non-associated flow rule, and an elastic behaviour definition. Formulations of the model are provided in the Appendix with surfaces illustrated in Fig. 2. The outer bounding surface restricts the allowable combination of vertical (V) and horizontal (H) load states for any embedment. Its size is determined by the bearing capacity of the pipe under pure vertical load (V_0).

With the UWAPIPE model simulating a small section of pipe-soil behaviour, a three-dimensional long pipeline can be modelled by attaching numerous force-resultant models. As illustrated in Fig. 3, the force-resultant model of UWAPIPE can be implemented into a structural finite element program as a point element. Details of the implementation of the UWAPIPE model into structural FE programs and the development of the time domain dynamic lateral stability analysis can be found in Tian and Cassidy (2010), Tian *et al.* (2010b) and Youssef *et al.* (2010).

3. Numerical scheme of uplifting and reattachment

The expansion of the combined loading yield surface of force-resultant plasticity models is commonly related directly to the plastic vertical displacement through the defined hardening law (see Schotman 1989, Martin and Houlsby 2001, Houlsby and Cassidy 2002, Cassidy *et al.* 2002, 2004, 2005 for example). Similarly, in UWAPIPE, an expanding bounding surface is accommodated with additional pipe penetration and bounding surface contraction is also possible with pipe heave. This is illustrated in Figs. 4(b) and 4(c) respectively and defined numerically by Eq. (3) in the Appendix. With the size of the bounding surface (V_0) shrinking with heave, a consistent criteria for pipe uplift is the outer bounding surface reducing to a point ($V_0 \rightarrow 0$). Numerically a tolerance should be used to account for this uplift, which is based on the largest recorded V_0 during loading history. A value of 10^{-6} of the maximum V_0 is used as the tolerance in the examples of this paper. Once the model shrinks below this tolerance the pipe is assumed to lose contact with the seabed. The model detaches and becomes numerically inactive. Under these conditions the stiffness contribution of the model is zero and the pipe can be considered to be a free structural node.

Under purely vertical uplift the tensile capacity of $-\beta V_0$ is first predicted before the capacity reduces to zero and the pipe lifts off the seabed as shown in Fig. 2. Under combination of horizontal load and vertical uplift, the combined 'bubble' and bounding surface retract towards zero, with both horizontal and vertical load capacity reducing during this process. In the illustrative example shown in Fig. 5, the pipe is first loaded to a value higher than its self-weight (i.e., path A→B) and numerically the UWAPIPE model establishes a surface of ⓑ. It is then unloaded to its

(a) Initial status

(b) Penetration:
Expansion of bounding surface
V_0 increasing

(c) Uplift:
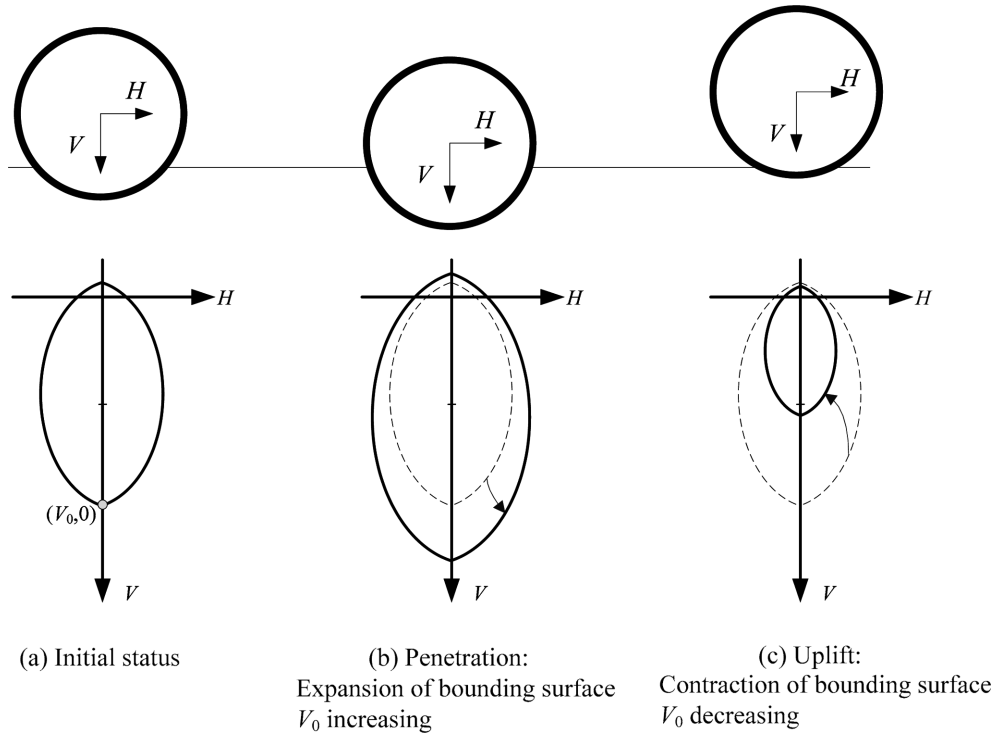Contraction of bounding surface
V_0 decreasing

Fig. 4 Illustration of bounding surface expansion and contraction with (a) penetration and (b) uplift of pipe
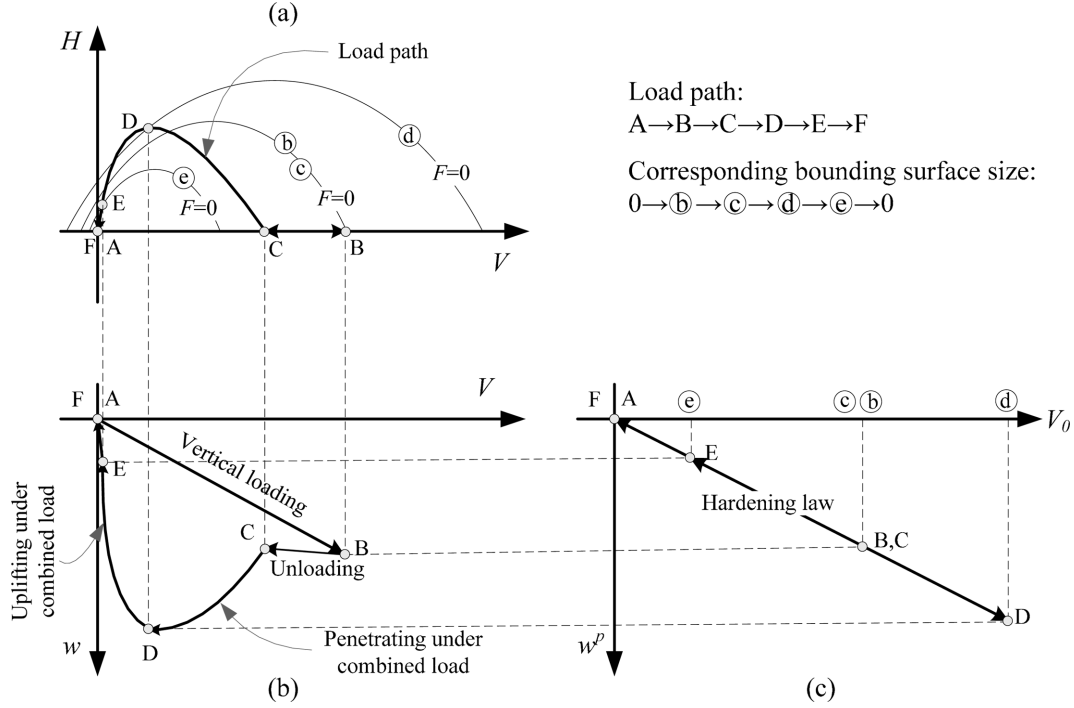
Fig. 5 Illustration of numerical scheme used in pipe uplift

self-weight (i.e., path B→C) and the bounding surface only slightly reduced due to the elastoplastic behaviour introduced by the 'bubble' (the bounding surface ⓒ is slightly smaller than ⓑ). Under a combined increasing horizontal and vertical hydrodynamic load the pipe possibly first undergoes a penetration and numerical expansion of the bounding surface before finally starting to uplift. This is shown in Fig. 5 as path C→D (the pipe penetrates with the bounding surface expands to ⓓ) followed by path D→E→F (pipeline uplifting occurs and the bounding surface is shrinking through ⓔ and finally to zero). At the end of the process, the pipe is uplifted completely from the seabed. Thus, the model becomes inactive and bounding surface contracts to a point. When incorporated in a structural finite element program, the stiffness matrix of the inactive model (uplifted clear of the seabed) becomes zero with no contribution to the global stiffness matrix.

　Two scenarios for the model reactivation are considered in this paper, as illustrated in Fig. 6. In the first, the pipe touches the surface within a horizontal zone where the model had previously been loaded. The pipe's previous movements are recorded during the analysis as minimum and maximum horizontal displacements, u_{min} to u_{max} respectively, as illustrated in Fig. 6. It is reasonable to assume that reattachment occurs at a vertical displacement equivalent to the maximum previously recorded plastic penetration w^P_{max}. When the model is reactivated the bounding surface is equal to the maximum size before uplift, and initial increments are considered to be elastic. The second scenario is that the pipe retouches an "unloaded" seabed outside of the u_{min} to u_{max} zone. In this situation the seabed is at the original surface (defined by pipe movement as $w = 0$) and the bounding surface starts from $V_0 = 0$ when the pipe touches it. It is acknowledged that both of these cases are simplifications of the seabed and soil behaviour, and do not account for issues such as the shape of any heaved material or berms established next to the pipe. Cyclic behaviour off and onto the seabed
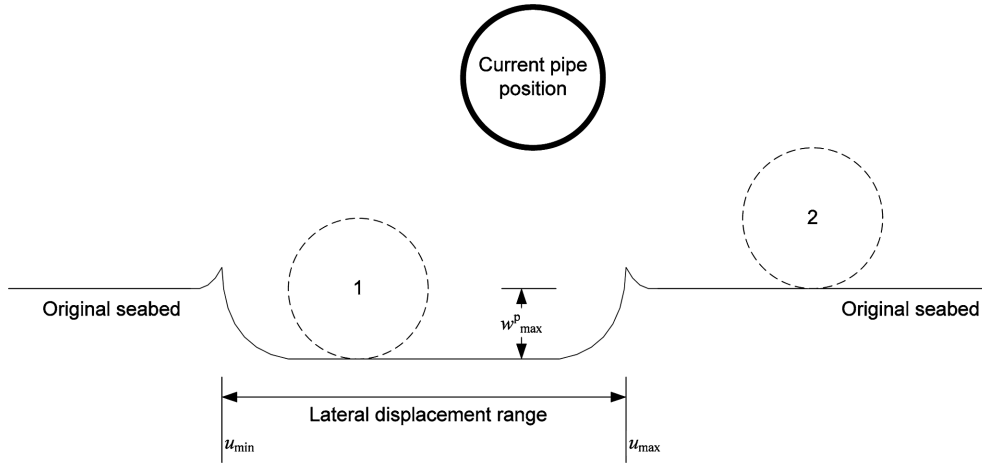
Fig. 6 Scenarios of reactivation

are also not accounted for in this proposal. Pumping of water between the pipe and seabed with repeated periodic movements could create an effective sediment transport mechanism to further erode the soil and effect behaviour (discussed for the application of steel catenary risers by Palmer 2000, Thethi and Moros 2001, Langner 2003), which is not being attempted here either.

4. Calculation examples

Three examples are presented to demonstrate and verify the methodology. The first two use only one UWAPIPE model to analyse a segment of pipe and the third uses 250 models to simulate a long pipeline. The first example acts as a verification of the numerical implementation of the above descried uplifting/reattachment methodology and the second is retrospectively simulated against centrifuge experiment of a segment of pipe. The third combines 250 UWAPIPE models to describe the behaviour of a 1245 m pipeline under complex storm conditions, which highlights the eventual application of the methodology.

Table 1 Model parameters

Parameter	Description	Value	Notes
k_{he}	Elastic stiffness (horizontal)	8000 kPa	Eq. (7)
k_{ve}	Elastic stiffness (vertical)	8000 kPa	Eq. (3), (7)
k_{vp}	Plastic stiffness (vertical)	200 kPa	Eq. (3)
β	Shape parameter representing tensile capacity	0.06	Eq. (1), (2)
κ	Increase of μ with normalised depth	0.65	Eq. (4)
μ_t	Shape parameter in the plastic potential equation	0.6	Eq. (6)
m	Exponent in the plastic potential equation	0.18	Eq. (6)
r	Size ratio of bubble to bounding surface	0.2	Eq. (2)

Note: Parameter values are as described by Zhang (2001), except the value of k_{vp} = 200 kPa. This is the best fit parameter for the centrifuge testing programme of Tian *et al.* (2009).

All of the analyses are run in ABAQUS with the UWAPIPE model written as a user element (known as an ABAQUS UEL). In the first two examples no structural pipe members are required as it is simply a pipe segment. In the third the pipeline is modelled by 249 ABAQUS beam column elements. Details of the implementation of UWAPIPE into ABAQUS as a UEL are provided in Tian and Cassidy (2010).

The UWAPIPE model parameters used in the analyses are provided in Table 1.

Example 1: Pipe segment with only vertical load and displacement

This example verifies the implementation of the numerical formulation to switch from active to inactive (and visa-versa). It is a simplified analysis with no horizontal force. After initially being laid the pipe is simulated to lift off the seabed surface and re-penetrate twice. The first is at the same horizontal coordinate (i.e., straight back down) and the second after being translated horizontally five metres above the seabed.

The computation results and the illustration of the loading process are shown in Fig. 7. Initially, the pipe segment is penetrated into the soil under the vertical load of 40 kN/m (A→B) and the bounding surface of $V_0 = 40$ kN/m is established at B. During the uplifting process (B→C), the size of the bounding surface shrinks and the model becomes inactive when the bounding surface size shrinks below the set tolerance. It can uplift unabated with no reaction until it reaches point D, chosen to be 0.1 m above the original seabed. On repenetration (D→E) into this seabed the size of the bounding surface is assumed to be its previous value of $V_0 = 40$ kN/m. This is a numerical assumption reflecting that the soil has densified during the previous embedment. Following further pipe penetration and bounding surface expansion (E→F $V_0 = 80$ kN/m), the pipe is again uplifted to 0.1 m above the seabed (F→G→H). The model again becomes inactive when the size of the

(a) Original position

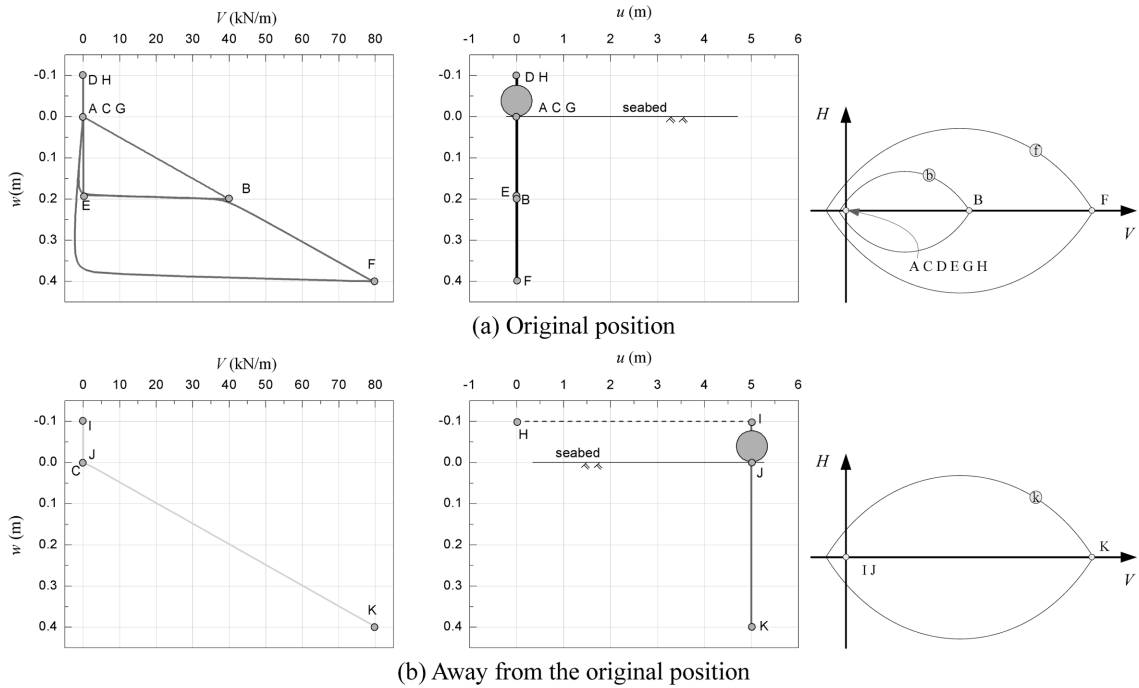(b) Away from the original position

Fig. 7 Numerical results of Example 1

bounding surface falls below the tolerance (at G). With a horizontal translation of 5 m (H→I, Fig. 7(b)) the pipe has moved away from the zone of loaded soil. When the model touches the seabed again the model starts anew with the size of the bounding surface expanding from $V_0 = 0$. From J→K, the pipe penetrates under increasing vertical load until 80 kN/m and the apex of the bounding surface expands to the same value (following the hardening law of Eq. (3)).

Example 2: Pipe segment subjected to horizontal translation and uplift at a constant ratio

To investigate the uplifting phenomenon, geotechnical centrifuge tests of a 20 mm diameter model pipe under 50-g accelerations were tested on the University of Western Australia's beam centrifuge (see Tian *et al.* 2009, 2010a for details). This represented a prototype pipe of 1 m diameter and 6 m in length. The tests were conducted on silty carbonate soils collected in 169 m water depth from the North West Shelf of Australia. Further details of the centrifuge tests are provided in Tian *et al.* (2008).

Accurately/modelling the behaviour of a pipe during simultaneously increasing drag and lift load is essential in the stability prediction of a pipe subject to hydrodynamic forces. The pipe was subjected to a combined horizontal translation and vertical uplift after initially being penetrated into the silty sand seabed in the centrifuge test. The steps of the test are given in Table 2. The pipe segment was first installed to a vertical load of 42.3 kN/m, approximately twice its assumed self-weight of 21.7 kN/m (Step 1 of Table 2). It was then unloaded back to a vertical load of 21.7 kN/m in Step 2. The pipe was then subjected to both horizontal and vertical uplift at a constant displacement ratio of $\Delta u/\Delta w = 1.3/(-0.088)$ in Step 3. The experiment loads measured are shown in Fig. 8(a)-(d). Initially the horizontal load increases before joining the vertical load in a gradual reduction (Fig. 8(c)).

This experimental test has been retrospectively simulated using the numerical UWAPIPE program. As shown in Fig. 8, the UWAPIPE model was subjected to the same steps, with load control used in Steps 1 and 2 and displacement control in Step 3. Steps 1 and 2 are a simulation of the process of pipe laying and unloading to self-weight. Step 3 uplifts and translates the pipe with a constant ratio with displacement control as shown Fig. 8(b) (noting that for the numerical simulation Step 3 is completed at point E on Fig. 8).

Fig. 9 shows the bounding surface established during this process. It expands to surface ⓑ ($V_0 = 42.3$ kN/m) from 0 in Step 1 (loading path A→B) and slightly reduces during Step 2 (B→C) as

Table 2 Loading steps in Example Problem 2

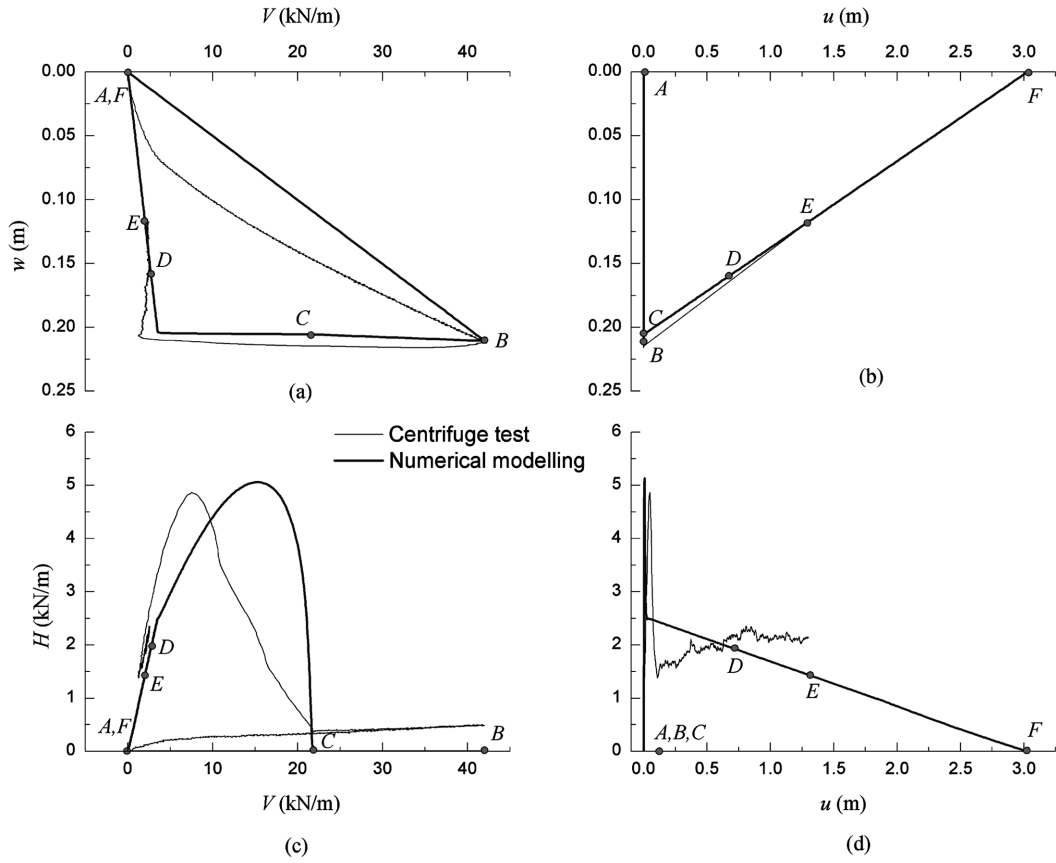| Step No.	Load Paths (Figs. 8 and 9)	Details		Numerical Bounding Surface (Fig. 9)		Note
				Beginning	End	
Step 1	A→B	V ↓ to 42.3 kN/m		A: $V_0 = 0$	B: $V_0 = 42.3$	Installation
Step 2	B→C	V ↑ to 21.7 kN/m		B: $V_0 = 42.3$	C: $V_0 \approx 42.3$	Unload to self-weight
Step 3	C→D→E	Δw ↑ 0.088 m	$\Delta u →$ 1.3 m	C: $V_0 \approx 42.3$	E: $V_0 \to 24.4$	Uplift with constant displacement path
Step 4	E→F	Δw ↑ 0.2 m (Numerical only)	$\Delta u →$ 3.0 m	E: $V_0 \approx 24.4$	F: $V_0 \to 0$	Loss of contact with surface

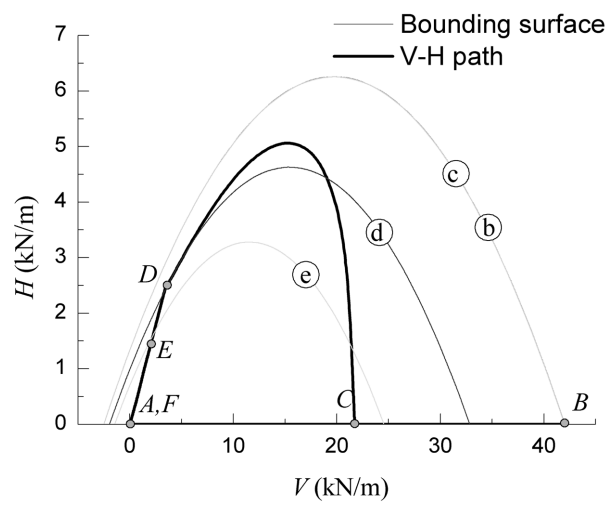Fig. 8 Comparison of centrifuge experiment and retrospective numerical simulation

Fig. 9 Bounding surface expansion in retrospective numerical simulation

only very small plastic displacements develop due to the kinematic hardening process (the bounding surface size ⓒ is almost same as ⓑ). In step 3, the bounding surface is contracting due to the loss of plastic penetration (load path is C→D→E and the bounding surface changing sequence is ⓒ→ ⓓ→ⓔ).

Due to physical space limitation within the centrifuge, the experiment was stopped before the footing removed itself from the seabed. Numerically this is represented by point E on Fig. 8 and until this point the UWAPIPE model is providing a close retrospective simulation of the experimental results. The numerical program translated the pipe further (Step 4 in Table 2), which provided evidence that the numerically formulation was able to detach when $V_0 \to 0$. This is shown as the loading path E→F in Fig. 8 and Fig. 9.

Example 3: Long pipeline under complex storm loading

This third example shows why modelling uplift for long pipelines subjected to large storms is required. It highlights that the methodology allows the three-dimensional time domain dynamic modelling of pipelines to numerically continue when only a segment of pipe is uplifted. It also shows the redistribution of loads that follows. The pipe simulated is typical of long gas pipelines currently being designed on the North West Shelf of Australia. A 1245 m pipeline with 250 structural nodes and 250 UWAPIPE models is analysed. This configuration is shown in Fig. 10. The pipeline is evenly divided into 249 beam elements with an element length of 5 m. The structural properties of the pipeline are listed in Table 3.

Hydrodynamic loads representing an example 1000 year return period of magnitude typical of North West Shelf conditions are applied to the model. Shown in Fig. 11 are the horizontal and vertical forces (F_h and F_v) acting on just one node. It should be noted that the load histories are different at each node due to spatial variation. In this case Node 39 has been randomly chosen for illustrative purposes. When combined with the self-weight of the pipe in Fig. 12 the resultant vertical force of the pipe segment at Node 39 is at times less than zero. The example highlighted is at time approximating 186s. It should be noted that the hydrodynamic loads used in this analysis were numerically generated using the Fourier model (Sorenson *et al.* 1986) rather than the
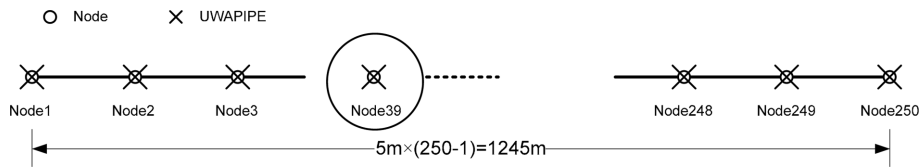

Fig. 10 Computation model used in Example Problem 3

Table 3 Structural properties of pipe used in Example 3

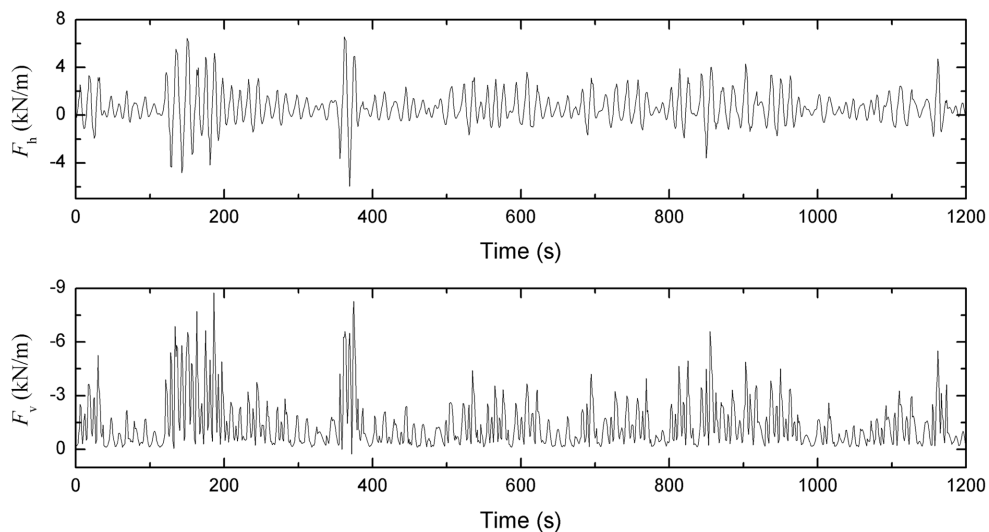| Parameter	Value
Outer diameter (m)	1.0
Wall thickness (m)	0.0312
Pipe submerged weight (empty) (kN/m)	7.6
Young's modulus of pipe (GPa)	210
Poisson's ratio of pipe	0.3

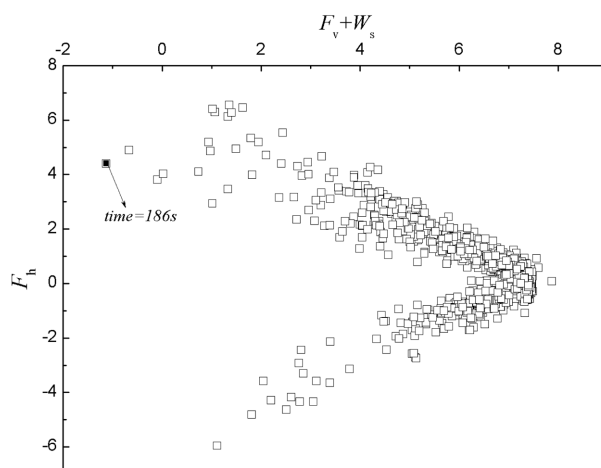Fig. 11 Hydrodynamic loading at example node

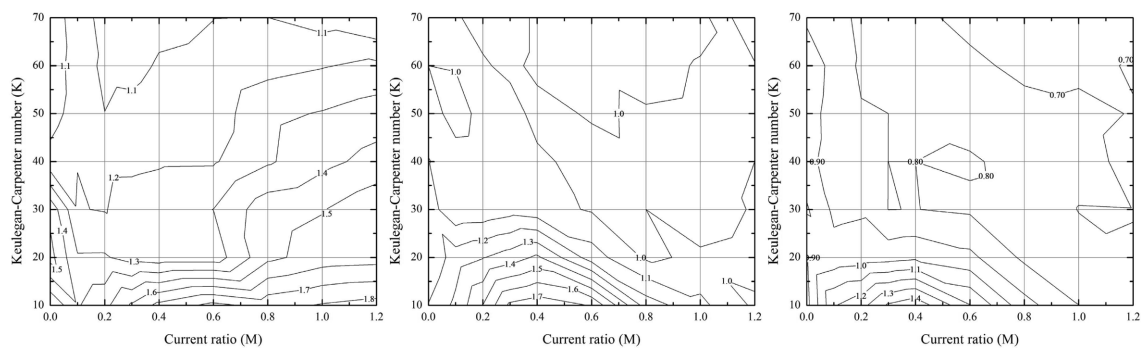Fig. 12 Combined hydrodynamic and gravitational vertical load at example node

Fig. 13 Ratio of lift to horizontal load (fine, medium and rough pipe surface)
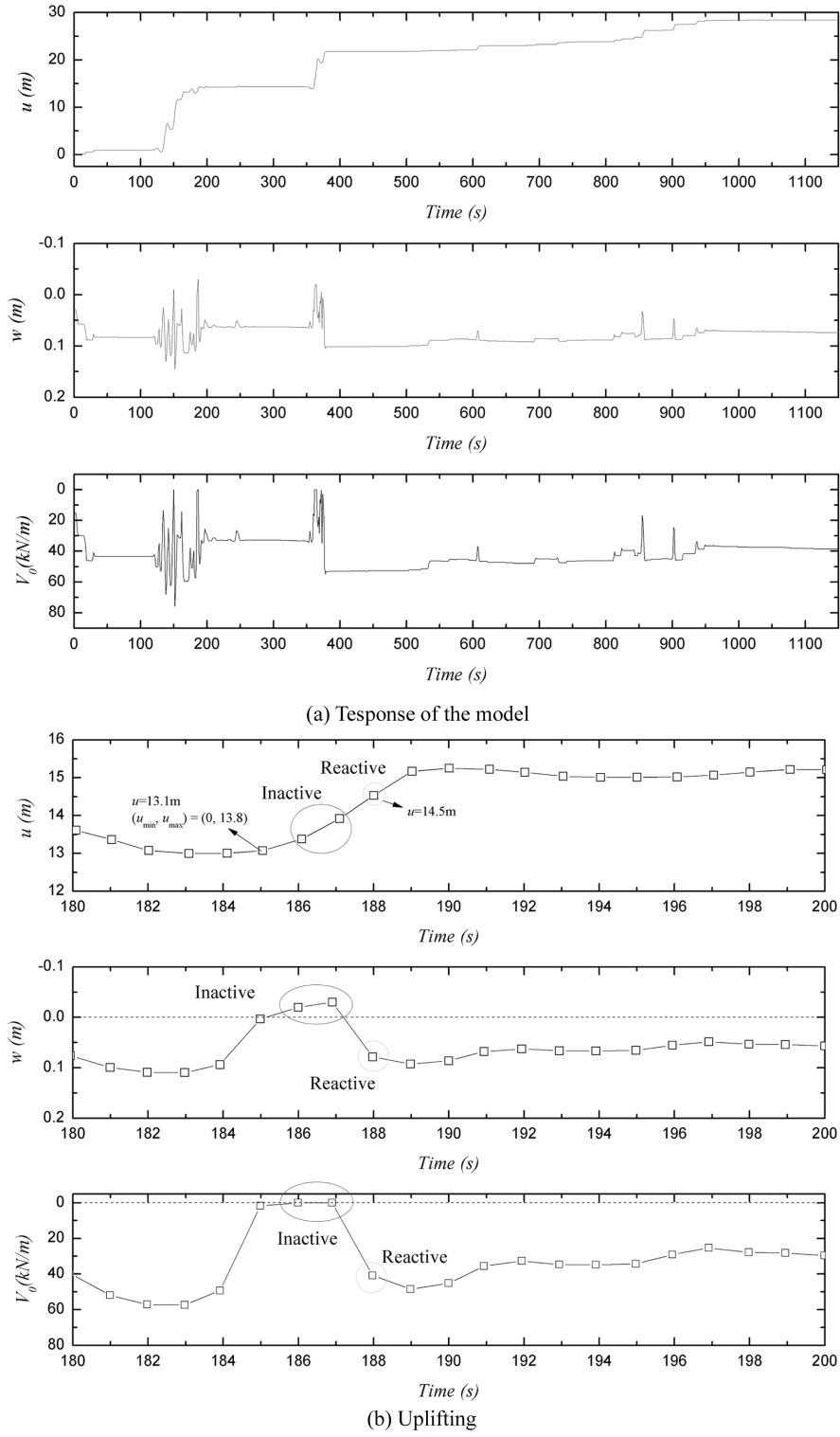
(a) Tesponse of the model

(b) Uplifting

Fig. 14 Interpretation of uplift and reattach (inactivation and reactivation)

traditional Morrison equation with a sea state derived from the JONSWAP spectrum (see Youssef *et al.* 2010 for details). Tian and Cassidy (2011a) recently investigated the ratio between lift force and horizontal force using the Fourier model, which is shown in Figs. 13(a)-(c) accounting for fine, medium and rough pipe surface.

Before the hydrodynamic loads are applied to the pipe the numerical simulation is initialised for the pipe-lay process. The peak vertical load during the pipe laying process was assumed to be 15.2 kN/m (twice the self-weight of 7.6 kN/m). This defines the initial size of the outer bounding surface V_0 in each of the UWAPIPE models. The pipe laying process was numerically simulated by load controlling the entire pipe to the peak load (expanding the surface with pipe penetration) before unloading to the self-weight. It is acknowledged that the pipe-laying process in the field may indeed be more complex with additional horizontal loads and even cyclic loading conditions applied to the

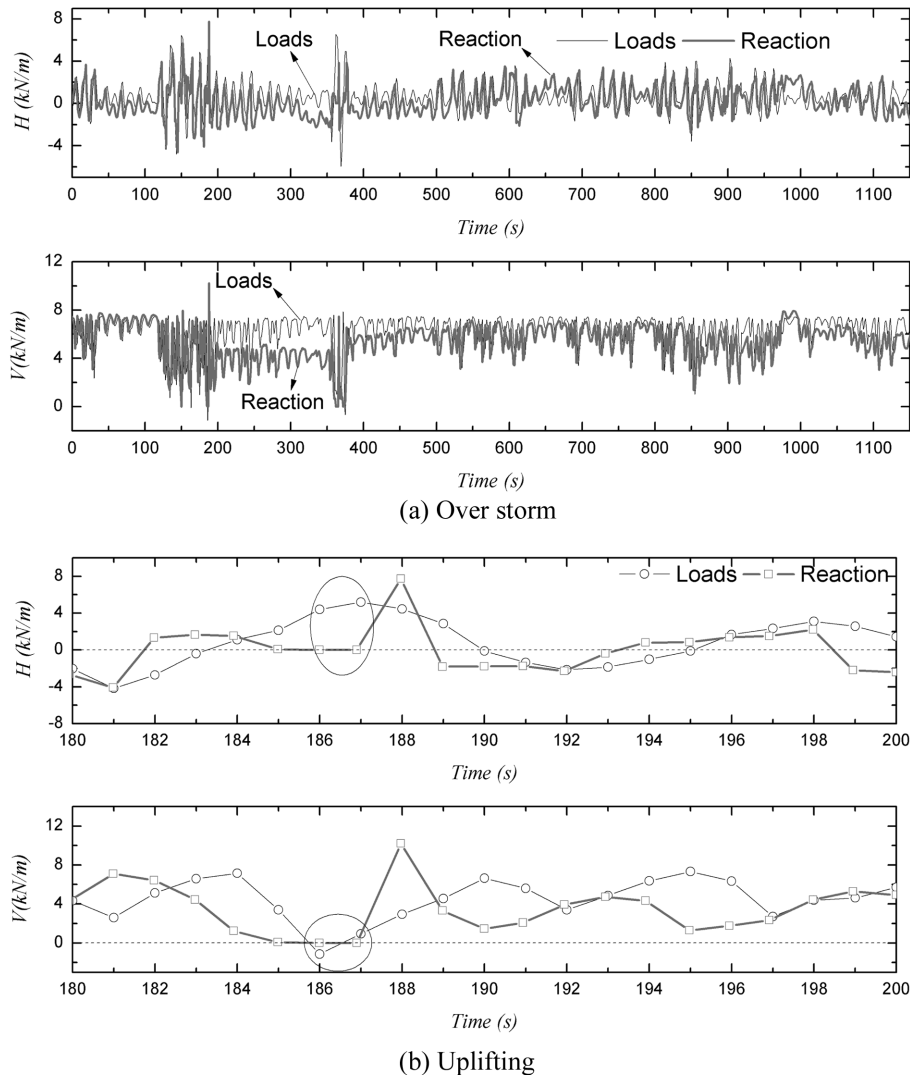(a) Over storm

(b) Uplifting

Fig. 15 Illustration of shedding loads

pipe. These are not included in the UWAPIPE model to date and represent a limitation of its capabilities.

The pipe displacements and model conditions evaluated for the storm loading are provided in Fig. 14. The lateral displacement (u), vertical penetration (w) and the size of the bounding surface (V_0) of the UWAPIPE model attached to Node 39 are shown in Fig. 14(a). Significant displacement occurred leading up to and during the uplift at ~186s. This is shown in more detail in Fig. 14(b), where the uplift and re-contact of the pipe are highlighted. At $t = 186$s, the pipe was uplifted ($w < 0$) and the UWAPIPE model at this node became inactive. This is shown in Fig. 14(b) by $V_0 = 0$. At this time the contribution of the UWAPIPE model to the pipeline stiffness and resistance at Node 39 is zero. At $t = 188$s, the pipe became active again. During the uplift event the pipe segment at Node 39 was displaced beyond the previous horizontal loaded region (u_{min}, $u_{max} = 0$, 13.8 m) (Fig. 14(b)). The hydrodynamic loads applied to Node 39 are compared with the reaction forces at the same node in Fig. 15(a). The results highlight that the reaction force V and H are not always the same as the applied loads. This is due to load shedding. It highlights one of the significant advantages of a three-dimensional time domain analysis. A simplified analysis of a plane strain segment of pipe would have to predict a failure when these diverge. The circled points of Fig. 15(b) show no reaction when the section of pipe is uplifted and the UWAPIPE model inactive. The hydrodynamic loading acting on this section of pipe is shared by the adjacent pipe sections that remain in the soil.

5. Limitations

This UWAPIPE is based on centrifuge tests to explain the force-displacement behaviour of shallowly embedded pipelines. Some other issues are not explicitly considered, such as the thermal buckling and earthquake loading as presented in Koike *et al.* (2007) and Paolucci *et al.* (2010) respectively. Both the original UWAPIPE and this proposed modification for uplifting conditions have modelling limitations.

For instance, the model has been developed from centrifuge data where the calcareous soils were in a drained condition. However, in the offshore condition fast loads such as hydrodynamics and thermal change can result in partially drained pipe soil behaviour. Wave-soil interaction can also cause accumulation of excess pore pressures in the soil surrounding the pipe. Further study is required to conduct centrifuge tests to account for displacement rate and partial drainage. It is also noted that the force-resultant model does not attempt to simulate all soil behaviour, with important considerations such as liquefaction or potential scour under the pipe not addressed in this drained model.

The original UWAPIPE model has been calibrated against experimental data for lateral displacement of up to five diameters (see Tian and Cassidy 2011b). However, the formulation avoids any detailed description of berm generation and potentially misses subtleties of pipe-soil behaviour. The modelling techniques described have only been derived from behaviour of a short pipe-segment measured in a geotechnical centrifuge. A major assumption is that when combined in a long pipe each can still adequately model different segments. Verification for a long length of pipe in offshore field conditions is still required and is of interest.

It is acknowledged that only one centrifuge test has been retrospectively simulated to test the uplift modifications presented in this paper. This does not represent a comprehensive evaluation of

the model under heaving conditions. Recent unit gravity model experiments on the lateral stability of pipelines, such as conducted by Gao *et al.* (2010), do provide further evidence of pipe uplift conditions and have potential use in model verifications. However, it is also recommended that further experiments that specifically follow the expected load paths of an offshore pipeline are conducted. Cyclic experiments load controlled along a particular offshore storm would also be most beneficial. However, this example provides a degree of confidence to this preliminary proposal.

6. Conclusions

This paper provides details of a model used to simulate the uplift of a shallowly embedded pipe in calcareous soils. A simple numerical methodology for detaching and reattaching a force-resultant model for the case of a pipe lifting off and returning back to the seabed is provided. It contributes to the knowledge in this field as all previous force-resultant models have only been applied to offshore problems requiring prediction of increasing capacity with footing penetration. However, in the calculation of on-bottom stability of unburied pipelines the opposite is required, as the uplift of the pipe can become significant with increasing storm severity. Without the ability to reduce stiffness and detach the pipe soil-model the three-dimensional structural analysis programs will terminate and stall.

The models use in a combined horizontal and reducing vertical load scenario is shown, with verification against experimental centrifuge results providing a degree of confidence in the use of the model in predicating behaviour during hydrodynamic uplifting events. Provision for reattachment of the numerical models under different assumptions of seabed conditions is also outlined. With the force-resultant model aimed at simulating the behaviour of long pipelines, the importance of providing for uplift under large storm loading was demonstrated for example seabed, pipeline and storm conditions of the coast of North West Australia. Under a spread sea only a segment of a pipeline will be uplift and there is the possibility of the load being resisted by neighbouring pipe that embeds further into the soil. Rather than defining uplift on a pipe segment as failure of an entire pipe, the ability to simulate the localised event and to continue the dynamic analysis is considered important. This paper provides a consistent methodology for conducting that type of analysis.

Acknowledgements

References

Bienen, B., Byrne, B.W., Houlsby, G.T. and Cassidy, M.J. (2006), "Investigating six-degree-of-freedom loading

of shallow foundations on sand", *Geotechnique*, **56**(6), 367-379.

Bienen, B. and Cassidy, M.J. (2009), "Three-dimensional numerical analysis of centrifuge experiments on a model jack-up drilling rig on sand", *Can. Geotech. J.*, **46**(2), 208-224.

Brennodden, H., Lieng, J.T. and Sotberg, T. (1989), "An energy-based pipe-soil interaction model", *OTC*, Houston, Texas.

Brown, N.B., Fogliani, A.G. and Thurstan, B. (2002), "Pipeline lateral stabilisation using strategic anchors", *Proceeding of the Society of Petroleum Engineers (SPE) Asia Pacific Oil and Gas Conference*, Melbourne, Australia.

Calvetti, F., Di Prisco, C. and Nova, R. (2004), "Experimental and numerical analysis of soil-pipe interaction", *J. Geotech. Geoenviron.*, **130**(12), 1292-1299.

Cassidy, M.J. (2006), "Application of force-resultant models in the analysis of offshore pipelines", *Struct. Eng. Mech.*, **22**(4), 511-515.

Cassidy, M.J. (2007), "Experimental observations of the combined loading behaviour of circular footings on loose silica sand", *Géotechnique*, **57**(4), 397-401.

Cassidy, M.J. (2011), "Assessing the three-dimensional response of jack-up platforms in directional seas", *KSCE J. Civil Eng., KSCE*, **15**(4), 623-634.

Cassidy, M.J., Airey, D.W. and Carter, J.P. (2005), "Numerical modelling of circular footings subjected to monotonic inclined loading on calcareous sands", *J. Geotech. Geoenviron.*, **131**(1), 52-63.

Cassidy, M.J., Byrne, B.W. and Houlsby, G.T. (2002), "Modelling the behaviour of circular footings under combined loading on loose carbonate sand", *Géotechnique*, **52**(10), 705-712.

Cassidy, M.J., Martin, C.M. and Houlsby, G.T. (2004), "Development and application of force resultant models describing jack-up foundation behaviour", *Marine Struct.*, **17**(3-4), 165-193.

Cathie, D.N., Jaeck, C., Ballard, J.C. and Wintgens, J.F. (2005), "Pipeline geotechnics – state-of-the-art", *Proceeding of the International Symposium on the Frontiers in Offshore Geotechnics: ISFOG 2005*, Perth, Taylor and Francis Group, Australia.

Di Prisco, C., Nova, R. and Corengia, A. (2004), "A model for landslide-pipe interaction analysis", *Soils Found.*, **44**(3), 1-12.

DNV (1981), *Rules for Submarine Pipeline Systems*.

DNV (1988), *On-Bottom Stability Design of Submarine Pipelines*, DNV-RP-E305.

DNV (2007), *On-Bottom Stability Design of Submarine Pipelines*, DNV-RP-F109.

Gaudin, C., Cassidy, M.J., Bienen, B. and Hossain, M.S. (2011), "Recent contributions of geotechnical centrifuge modelling to the understanding of jack-up spudcan behaviour", *Ocean Eng.*, **38**(7), 900-914.

Gottardi, G., Houlsby, G.T. and Butterfield, R. (1999), "Plastic response of circular footings on sand under general planar loading", *Geotechnique*, **49**(4), 453-469.

Hodder, M.S. and Cassidy, M.J. (2010), "A plasticity model for predicting the vertical and lateral behaviour of pipelines in clay soils", *Geotechnique*, **60**(4), 247-263.

Holthe, K., Sotberg, T. and Chao, J.C. (1987), "An efficient computer program for predicting submarine pipeline response to waves and current", *Proceedings of the 19th Offshore Technology Conference*, Houston, Texas.

Houlsby, G.T. and Cassidy, M.J. (2002), "A plasticity model for the behaviour of footings on sand under combined loading", *Geotechnique*, **52**(2), 117-129.

Koike, T., Maruyama, O. and Garciano, L.E. (2007), "Ground Strain Estimation for Lifeline Earthquake Engineering", *Struct. Eng. Mech.*, **25**(3), 291-310.

Langner, C.G. (2003), "Fatigue life improvement of steel catenary risers due to self-trenching at the touchdown point", *Proceeding 35th Offshore Technology Conference*, Houston, OTC 15104, USA.

Martin, C.M. and Houlsby, G.T. (2000), "Combined loading of spudcan foundations on clay: laboratory tests", *Geotechnique*, **50**(4), 325-338.

Martin, C.M. and Houlsby, G.T. (2001), "Combined loading of spudcan foundations on clay: numerical modelling", *Geotechnique*, **51**(8), 687-699.

Palmer, A. (2000), "Catenary riser interaction with the seabed at the touchdown point", *Proceeding of the Deepwater Pipeline and Riser Technology Conference*, Houston, USA.

Paolucci, R., Griffini, S. and Mariani, S. (2010), "Simplified Modelling of Continous Buried Pipelines Subject to Earthquake Fault Rupture", *Earthq. Struct.*, **1**(3), 253-267.

PRCI (2002), "Submarine pipeline on-bottom stability", PRCI. Project Number PR-178-01132.

Schotman, G.J.M. (1989), "The effects of displacements on the stability of jackup spudcan foundations", *Proceeding of the 21st Offshore Technology Conference*, Houston.

Sorenson, T., Bryndum, M. and Jacobsen, V. (1986), "Hydrodynamic forces on pipelines- model tests", Danish hydraulic Institute (DHI). Contract PR-170-185. Pipeline Research Council International Catalog No. L51522e.

Thethi, R. and Moros, T. (2001), "Soil interaction effects on simple catenary riser response", *Deepwater Pipeline and Riser Technology Conf.*, Houston, USA.

Tian, Y. and Cassidy, M.J. (2008), "Modelling of pipe-soil interaction and its application in numerical simulation", *Int. J. Geomech.*, **8**(4), 213-229.

Tian, Y. and Cassidy, M.J. (2010), "The challenge of numerically implementing numerous force-resultant models in the stability analysis of long on-bottom pipelines", *Comput. Geotech.*, **37**, 216-312.

Tian, Y. and Cassidy, M.J. (2011a), "Equivalent absolute lateral static stability of on-bottom offshore pipelines", *Marine Struct,.* (under review, submitted on 6 May 2011)

Tian, Y. and Cassidy, M.J. (2011b), "A pipe-soil interaction model incorporating large lateral displacements in calcareous sand", *J. Geotech. Geoenviron.*, **137**(3), 279-287.

Tian, Y., Cassidy, M.J. and Gaudin, C. (2008), "Centrifuge tests of shallowly embedded pipeline on silt sand", GEO:09475 Report of Centre for Offshore Foundation Systems, the University of Western Australia.

Tian, Y., Cassidy, M.J. and Gaudin, C. (2010a), "Advancing pipe-soil interaction models through geotechnical centrifuge testing in calcareous sand", *Appl. Oceon Res.*, **32**(3), 294-297.

Tian, Y., Cassidy, M.J. and Youssef, B.S. (2010b), "Consideration for on-Bottom Stability of Unburied Pipelines Using Force-Resultant Models", *The 20th International Offshore (Ocean) and Polar Engineering Conference*, Beijing, China.

Tørnes, K., Zeitoun, H., Cumming, G. and Willcocks, J. (2009), "A stability design rationale - a review of present desgin approaches", *Proceedings of the ASME 2009 28th International Conference on Ocean, Offshore and Arctic Engineering*, Honolulu, Hawaii, USA.

Verley, R.L.P. and Lund, K.M. (1995), "A soil resistance model for pipelines placed on clay soils", *Proceedings of the International Offshore Mechanics and Arctic Engineering Symposium.*

Verley, R.L.P. and Sotberg, T. (1992), "Soil resistance model for pipelines placed on sandy soils", *Proceedings of the International Offshore Mechanics and Arctic Engineering Symposium.*

Wagner, D.A., Murff, J.D., Brennodden, H. and Sveggen, O. (1989), "Pipe-soil interaction-model", *J. Waterw. Port C-ASCE,* **115**(2), 205-220.

Wantland, G.M., O'Neill, M.W., Reese, L.C. and Kalajian, E.H. (1979), "Lateral stability of pipelines in clay", *Proceedings of the 11th Annucal OTC*, Houston, Texas.

Youssef, B.S., Cassidy, M.J. and Tian, Y. (2010), "Balanced three-dimensional modelling of the fluid-structure-soil interaction of an untrenched pipeline", *Proceeding of the 20th International Offshore (Ocean) and Polar Engineering Conference* Beijing, China.

Zeitoun, H., Tørnes, K., Cumming, G. and Brankoviæ, M. (2008), "Pipeline stability - state of the art", *Proceedings of the ASME 27th International Conference on Offshore Mechanics and Arctic Engineering*, Estoril, Portugal.

Zeitoun, H., Tørnes, K., Li, J., Wong, S., Brevet, R. and Willcocks, J. (2009), "Advanced dynamic stability analysis", *Proceedings of the ASME 2009 28th International Conference on Ocean, Offshore and Arctic Engineering*, Honolulu, Hawaii, USA.

Zhang, J. (2001), "Geotechnical stability of offshore pipelines in calcareous sand", University of Western Australia.

Zhang, J., Stewart, D.P. and Randolph, M.F. (2002a), "Kinematic hardening model for pipeline-soil interaction under various loading conditions", *Int. J. Geomech.*, **2**(4), 419-446.

Zhang, J., Stewart, D.P. and Randolph, M.F. (2002b), "Modelling of shallowly embedded offshore pipelines in calcareous sand", *J. Geotech. Geoenviron.*, **128**(5), 363-371.

Appendix: Review of the formulation of the UWAPIPE model

UWAPIPE includes three models with increasing sophistication. Only the most advanced two-yield surface kinematic hardening model is used in this paper. This model comprises of four components: an outer bounding surface and an inner yield or colloquially called "bubble" surface; isotropic and kinematic hardening laws; a non-associated flow rule and an elastic behaviour definition. The small inner "bubble" yield surface travels inside the outer bounding surface according to the kinematic hardening law (refer to Fig. 2 for illustration). The constitutive behaviour of the models is described briefly by the following equations. Parameter definition and values adopted in this paper are provided in Table 1.

Bounding surface and bubble surface
The equations for the bounding and bubble surfaces are written directly in terms of the load on the model

$$F = |H| - \mu\left(\frac{V}{V_0} + \beta\right)(V_0 - V) = 0 \tag{1}$$

$$f = |H - H_N| - \mu\left(\frac{V - V_N}{rV_0} + \frac{1+\beta}{2}\right)\left(\frac{1+\beta}{2}rV_0 - (V - V_N)\right) = 0 \tag{2}$$

where $F = 0$ is the outer bounding surface and $f = 0$ is the inner bubble surface; μ, β are aspect ratios defining the surface shape and V_0 is the size of the bounding surface representing the bearing capacity of the pipe under purely vertical load at the current embedment; the subscript N denotes the bubble centre (as shown by the cross in Fig. 2) and r is the size ratio of the bubble to the bounding surface. The surfaces are illustrated in Fig. 2.

Hardening law
Hardening of the surfaces occurs by (i) isotropic hardening of the outer bounding surface and (ii) kinematic hardening of the inner bubble surface. The former is directly correlated to the vertical plastic displacement increment Δw^p as a change in surface size as

$$\Delta V_0 = \frac{k_{ve}k_{vp}}{k_{ve} - k_{vp}}\Delta w^p \tag{3}$$

$$\Delta\mu = \frac{\kappa}{D}\Delta w^p \tag{4}$$

where the superscript p denotes a plastic component; κ is the slope of μ to w^p; D is the pipe diameter. k_{ve} and k_{vp} are the elastic and plastic vertical stiffness, respectively. Kinematic hardening of the bubble surface is determined by

$$\Delta\mathbf{F}_N = \Delta\mathbf{F}_M + \left(\frac{\Delta V_0}{V_0} + \frac{\Delta\mu}{\mu}\right)\frac{1-r}{r}(\mathbf{F} - \mathbf{F}_N) + \Delta\Lambda(\mathbf{F}_C - \mathbf{F}) \tag{5}$$

where the subscript *M, N, C* represent the bounding surface centre, bubble center and the conjugate point of the current force respectively (and these are labeled on Fig. 2). $\mathbf{F} = \{V, H\}^T$ is the force vector. The scalar $\Delta\Lambda$ can either be explicitly evaluated according to the consistency condition of the bubble surface or be implicitly iterated to integrate the constitutive equations (Tian and Cassidy 2010). The bubble surface translates smoothly inside of but never intersects or lies outside of the bounding surface.

Flow rule
Based on experimental evidence a non-associated flow rule is required. It is formulated so that the plastic potential surface maintains a similar shape and position with the bubble surface.

$$g = |H - H_N| - \mu_t\left(\frac{V}{V_0} + \beta\right)^m (V_0 - V) = 0 \tag{6}$$

where μ_t and m are aspect ratios controlling the shape of the plastic potential surface.

Elasticity

For increments inside the bubble surface, the elastic relationship of the model is

$$\Delta\mathbf{F} = \begin{Bmatrix} \Delta V \\ \Delta H \end{Bmatrix} = \mathbf{D}^e \Delta\mathbf{U}^e = \begin{bmatrix} k_{ve} & 0 \\ 0 & k_{he} \end{bmatrix} \begin{Bmatrix} \Delta w^e \\ \Delta u^e \end{Bmatrix} \tag{7}$$

where $\mathbf{U} = \{w, u\}^T$ is the force and displacement vectors; k_{he} is the horizontal elastic stiffness; Δ represents an increment and the superscript e denotes an elastic component.

Elastoplastic matrix

The constitutive relationship of the model can be written as

$$\Delta\mathbf{F} = \begin{Bmatrix} \Delta V \\ \Delta H \end{Bmatrix} = \mathbf{D}^{ep} \Delta\mathbf{U}^e = \left(\mathbf{D}^e - \frac{\mathbf{D}^e \dfrac{\partial f}{\partial \mathbf{F}}^T \dfrac{\partial g}{\partial \mathbf{F}} \mathbf{D}^e}{K + \dfrac{\partial f}{\partial \mathbf{F}}^T \mathbf{D}^e \dfrac{\partial g}{\partial \mathbf{F}}} \right) \begin{Bmatrix} \Delta w \\ \Delta u \end{Bmatrix} \tag{8}$$

where K is plastic modulus.